SEMI-QUANTITATIVE IDENTIFICATION OF COLOUR ASSOCIATED GULLY CHANGES THROUGH CASSIS BAND RATIOS AND SPECTRAL ANALYSIS TECHNIQUES. V. G. Rangarajan[1], L. L. Tornabene[1], G. R. Osinski[1], F. P. Seelos[2], S. J. Conway[3], C. M. Dundas[4], M. R. Patel[5], N. Thomas[6], G. Cremonese[7], M. Pajola[7], A. Lucchetti[7], G. Munaretto[7,8] and the CaSSIS Team. [1]Institute for Earth and Space Exploration/ Dept. of Earth Sciences, University of Western Ontario, London, ON, Canada (vrangara@uwo.ca) [2]Applied Physics Laboratory, John Hopkins University, Laurel, MD, USA [3]CNRS Laboratoire de Planétologie et Géodynamique de Nantes, CNRS UMR 6112, Université de Nantes, France [4]U.S. Geological Survey, Astrogeology Science Center, Flagstaff, AZ, USA [5]School of Physical Sciences, STEM, The Open University, Milton Keynes, UK [6]Physikalisches Institut, University of Bern, Sidlerstr. 5, 3012 Bern, Switzerland [7]INAF-Osservatorio Astronomico di Padova, Padova, Italy [8]Department of Physics and Astronomy, University of Padova, Padova, Italy.

Introduction: Gullies are one of the most studied active surface processes on Mars. Their regular tracking through high spatial and temporal scale observations is critical to help constrain timelines of activity, and by extension, provide glimpses into past and present climate cycles that played a role in their formation [1-4]. Observations from the High Resolution Imaging Science Experiment (HiRISE) [5] and the Context Camera (CTX) [6] onboard the Mars Reconnaissance Orbiter (MRO) have been largely used to identify and document these features. More recently, combinations of images from the Colour and Stereo Surface Imaging System (CaSSIS) [7] onboard the ExoMars Trace Gas Orbiter (TGO) along with simulated CaSSIS images based on MRO datasets [8] have proven their utility for such campaigns, owing to their extensive four-band colour swath, compared to the narrow HiRISE colour strip [9]. So far, most identifications of new changes have been based on qualitative visual comparisons of pre- and post-images across timelines. However, this poses some challenges when dealing with images taken under different atmospheric and geometric conditions, as variable image acquisition parameters can significantly affect interpretations. This work presents initial findings of a set of additional quantitative colour-based techniques that can be used in concert with visual comparison methods, to aid reliable identifications of new changes between images.

Data and Methods: Gasa crater (-35.7N, 129.4E), host to one of the most active gully systems on Mars [10], is the primary focus of this study. Three fully simulated CaSSIS cubes and one actual CaSSIS image (MY34_005684_218_1) were used for this analysis [9], with the simulated cubes (with IDs based on CRISM: 06220, 13F9F and 1E5A2) produced by combining coordinated CRISM and CTX observations. Figures 1a and 1b show HiRISE RED images of a new gully deposit formed in early MY30. This change was initially missed by the colour swath of HiRISE, and had to be specifically targeted in later cycles to derive associated colour information. Figures 1c and 1d show corresponding colour infrared simulated CaSSIS composites exhibiting a distinctive blue colour associated with the new deposit. This distinct colour infrared signature is characteristic of most new changes seen at Gasa [4, 8-10].

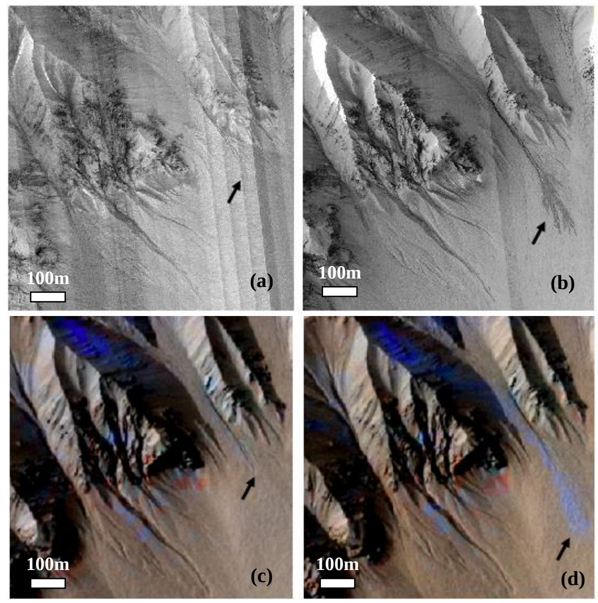

Figure 1. A pair of HiRISE RED (a and b) and simulated CaSSIS NIR-PAN-BLU composite images (c and d) showing the formation of a gully deposit in the northwestern portion of Gasa crater in early MY30. Images shown here are (a) ESP_018327_1440 (b) ESP_019461_1440 and simulated products dubbed (c) 13F9F and (d) 1E5A2, after the CRISM IDs they were produced from.

Apart from visual comparison of each CaSSIS product, we also employ three additional techniques, described below, to identify gully changes.

***Method 1 - Computation of ferric/ferrous ratios to separate new deposits from background*:** Most new gully deposits at Gasa are comparatively more ferrous in composition than the surrounding ferric surfaces [4, 8, 9]. Hence, we use a set of four ratios strategically developed to enhance the ~1000nm and ~500nm absorptions associated with ferrous- and ferric-bearing materials, respectively [8]. To gauge the accuracy of these ratios, 10 locations were chosen along the crater floor, where no change had occurred between successive images. Mean differences for the four ratios between two images at these points were computed to identify the minimum ratio value that constitutes a real colour change (Least Count (L.C.) in Table 1), thus providing a reasonable way to eliminate false positive detections.

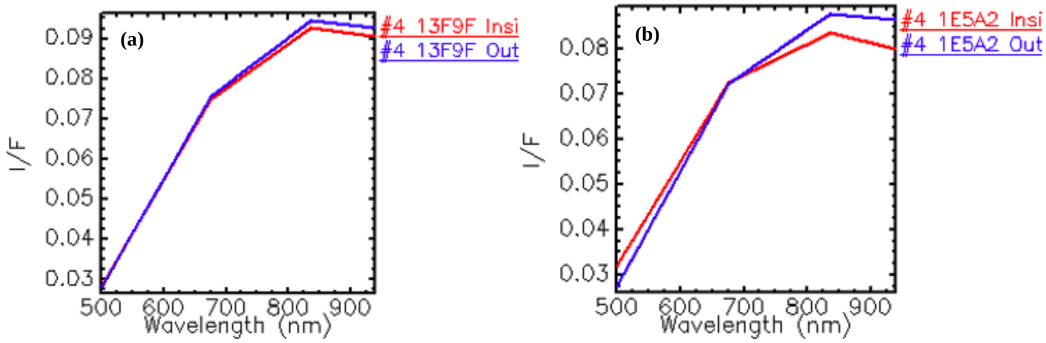

Figure 2. Comparison of spectra taken from ROIs inside (red) and outside (blue) the change region. (a) shows these spectra for the pre-change image (13F9F) while (b) shows the spectra for the post-change image (1E5A2)

Method 2 - Direct spectral comparison between pre- and post-change images: In this method, spectra were extracted from a Region of Interest (ROI) within the area of change and were compared between pre- and post-change images. To reduce effects of atmospheric contributions on image scenes, a dark object subtraction technique was employed prior to extraction of spectra.

Method 3 - In-scene spectral comparison of change and non-change regions in pre- and post-change images: In this technique, spectra were extracted and compared from two ROIs – one inside and one just outside the change area, for both pre- and post-change images. It is critical that both ROIs are taken at locations of similar slope, so that illumination/topographical effects are reduced [11]. Since spectral comparison takes place within the same image, this method is unaffected by varying image acquisition parameters between pre- and post-change scenes.

Results: A total of 22 changes (15 new and 7 fading) were observed from the set of simulated and actual CaSSIS products. An observed increase in PAN/NIR and decreases in PAN/BLU, RED/PAN and NIR/BLU appear to correlate with pre- and post-image changes for new deposits (Table 1); this is consistent with new gully deposits being more ferrous in composition than surrounding ferric surfaces.

Table 1 List of values and least counts (L.C.) obtained for each of the four CaSSIS ratios for the change shown in Figure 1

Ratios	13F9F	1E5A2	L.C.
PAN/NIR	0.833	0.905	0.012
PAN/BLU	2.648	2.277	0.081
RED/PAN	1.232	1.151	0.020
NIR/BLU	3.172	2.516	0.141

For fading changes, presumably from deposition of airborne ferric dust particles over time, a decrease in the PAN/NIR ratio is observed with increases in PAN/BLU, RED/PAN and NIR/BLU. Ambiguous colour changes seen in the CaSSIS products, that may not be indicative of a real feature, showed no significant changes in ratio values. This helped separate false positives from actual colour changes, based on a qualitative assessment alone.

Constraining differences in pre- and post-image spectra was found to be particularly challenging; this is likely due to variations in atmosphere and illumination between scenes and their influences on I/F values, rendering inter-image comparison unreliable. On the other hand, in-scene comparison of spectra between change and non-change regions on similar slopes, provides a plausible alternative to quantitatively characterize colour surface changes (Figure 2).

Conclusions: Initial results from this work indicate that at least two of the three techniques seem to be effective for new change detections, and may enable identification in cases where corresponding HiRISE images may not be readily available. Some changes like the one in Figure 1, that are basically invisible in HiRISE RED, can also be readily detected through these colour-based techniques, hence aiding confirmation when high-resolution colour information is unavailable. To understand the limits of using such ratios and spectral comparisons for future gully change detection across Mars, analysis is currently underway on other gully monitoring sites that exhibit ferrous and non-ferrous colour changes.

References: [1] Malin and Edgett (2000), *Science 288* [2] Head et al. (2008), *PNAS 105(36)* [3] Dickson et al. (2015), *Icarus 252* [4] Dundas et al. (2019), *Geol. Soc. 467(1)* [5] McEwen et al. (2007), *JGR 112* [6] Malin et al. (2007), *JGR 112* [7] Thomas et al. (2017), *SSR 212* [8] Tornabene et al. (2018), *SSR 214(18)* [9] Rangarajan et al. (2020), *EPSC 2020-475* [10] Harrison et al. (2019), *Geol. Soc. 467(1)* [11] Munaretto et al. (2020), *PSS 187.*

Acknowledgments: We thank the spacecraft and instrument engineering teams for the successful completion of the instrument. CaSSIS is a project of the University of Bern and funded through the Swiss Space Office via ESA's PRODEX programme. The instrument hardware development was also supported by the Italian Space Agency (ASI), INAF/Astronomical Observatory of Padova, and the Space Research Center (CBK) in Warsaw. Support from SGF (Budapest), the University of Arizona (Lunar and Planetary Lab) and NASA are also acknowledged. The lead author acknowledges support from Tornabene's funding from the CSA's Planetary and Astronomy Missions Co-Investigator programme (19PACOI07) and the Canadian NSERC Discovery Grant programme (06418-2020 RGPIN). CMD was funded by MDAP.